ON NONLINEAR STIFFNESS OF THE SLEEVE ACTUATOR

ADRIAN IOAN NICULESCU

Abstract. The paper presents the stiffness evolution with the stroke, in pneumatic sleeve actuator, gives the elements implied in it and thus the possibility to adjust it. When the actuator has closed all connections with the outside, the volume variation with the stroke is strongly affected and thus the inner pressure generates nonlinear actuator stiffness and thus the suspension behavior. A slow stiffness growing has a good effect by reducing the number and amplitude of the suspension limiter bumper collisions on compression, but a big stiffness growing will increase strongly the gas pressure generating inner tensions, above the mechanical resistance in the pneumatic components. To avoid these inconveniences the paper defines each element implied in stiffness evolution and expresses the pressure and stiffness evolution with the stroke, in function of the initial gas pressure. For better understanding, the paper shows images of the system in each main position and presents result tabular and by diagram.

Key words: sleeve actuator, pressure, stiffness.

1. ABOUT THE RUBBER SLEEVE ACTUATOR

The sleeve actuator is a consecrate pneumatic rubber actuator solution, some realisation versions being presented in papers [1–5].

The sleeve actuator works together a shock absorber on whose upper part of the outer cylinder and on a lid fastened on the upper ending rod fasten a rubber reinforced sleeve. The sleeve actuator has advantage of a slow air chamber volume variation with the stroke, this assuring a reduced pneumatic stiffness variation with the stroke. Instead, the sleeve actuator has disadvantage of sensibility to debris, to low resistance at a high number of sleeve rolling and especially when uses on steering axles where spinning generates earlier cracks.

Figure 1 shows the sleeve actuator in the main working situation *e.g*. Fig. 1a shows the actuator in fully extended position, Fig. 1b shows the situation when start the bumper collision and Fig. 1c when the bumper is fully compressed.

The actuator is dived in three zones, zone 1 defined by the bottom sleeve

Institute of Solid Mechanics of the Romanian Academy, Bucharest, Romania

Ro. J. Techn. Sci. – Appl. Mechanics, Vol. 67, N° 2, P. 197–206, Bucharest, 2019

part, zone 2 representing the area of free actuator stroke and zone 3 including the area of compression stopper bumper. Each three zones are variable with the actuator stroke.

The model elements presented in Fig. 1 are explained in Table 1.

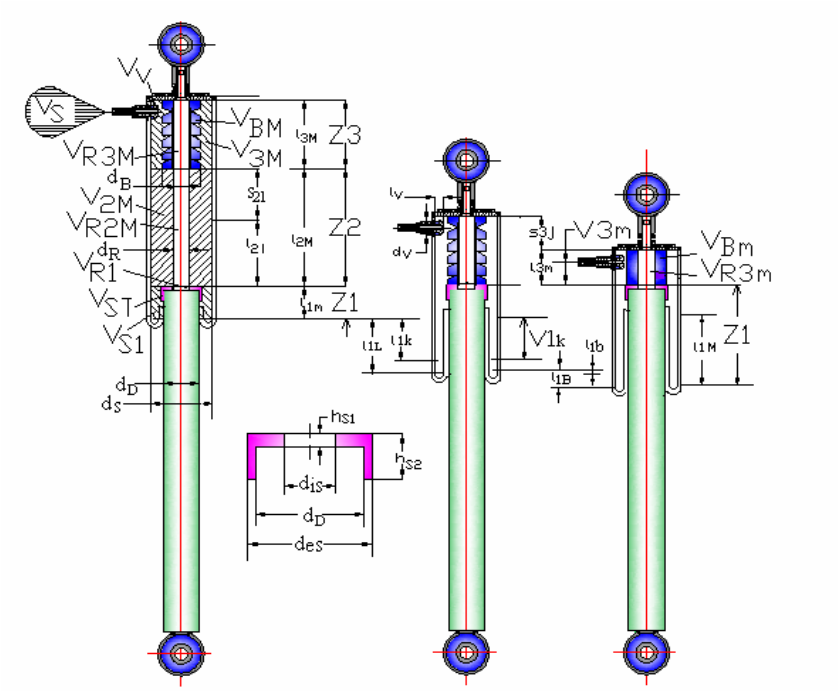

Fig. 1–Actuators: a) actuator in maximal extension; b) actuator at free stroke ending, c) actuator in minimal extension.

Table 1

The model elements

Element	Signification	Element	Signification
Z1	Zone 1	V_{3j}	Gas volume, zone 3, position "*j*"
Z2	Zone 2	V_{3M}	Maximum gas volume in zone 3
Z3	Zone 3	V_{3m}	Minimum gas volume in zone 3
V_T	Actuator total gas volume	V_{T3j}	Total gas volume in position "*j*" from zone 3
V_{TM}	Actuator maximal gas volume	V_{3j}	Gas volume in zone 3, for position "*j*"
V_{Tm}	Actuator minimal gas volume	V_{BM}	Compression bumper volume uncompressed

Element	Signification		Element	Signification
V_1	Gas volume in zone 1		V_{Bm}	Compression bumper volume compressed
V_{1m}	Gas volume in zone 1 for l_{1m}		V_V	Volume of valve fastening part
V_{R1}	Rod volume in zone 1		$V_{R3\,j}$	Rod volume in zone 3
V_{TS}	Toric stopper bumper volume		V_{R3M}	Maximal rod volume in zone 3
V_{1k}	Volume of 1 zone for s_{1k}		V_{R3m}	Minimal rod volume in zone 3
V_{1B}	Volume of 1 zone for s_{1B}		V_{T3m}	Minimal gas volume in zone 3
l_1	Sleeve length in zone 1		V_{Tm}	Minimal gas volume all zones
l_{1m}	Minimal sleeve length in zone 1		V_{S1}	Volume of sleeve in zone 1
l_{1k}	Sleeve stroke for position *k*		$s_{3\,j}$	Bumper deformation with stroke "*j*"
l_{1L}	Sleeve stroke at bumper attack		s_{3M}	Maximal bumper deformation
l_{1M}	Maximal sleeve length in zone 1		$l_{3\,j}$	Bumper length in situation "*j*"
l_{1b}	Sleeve stroke for bumper deformation with "s_{3j}"		l_{3M}	Maximal value of "l_{3j}"
l_{1B}	Sleeve stroke for bumper maximum deformation		$p_{3\,j}$	Pressure for position "*j*"
V_{1k}	Sleeve volume in area "*k*"		d_S	External sleeve camera diameter
V_{1b}	Gas volume - zone 1 position "*b*"		d_R	Rod diameter
V_S	Supplementary elements volume		d_D	External damper diameter
V_{2i}	Gas volume in zone 2		d_B	Bumper diameter
V_{2M}	Maximum gas volume in zone 2		p_0	Minimal gas pressure
V_{2m}	Minimum gas volume in zone 2		p_M	Maximal gas pressure
V_{T2i}	Total gas volume in position "*i*" from zone 2		p_{3M}	Maximal gas pressure in zone 3
V_{R2i}	Rod volume in zone 2		l_1	Length of bottom sleeve – area 1
V_{R2M}	Maximal rod volume in zone 2		l_m	Minimal length of bottom sleeve
V_{R2m}	Minimal rod volume in zone 2		l_{1M}	Maximal length of bottom sleeve
s_{2i}	Stroke in situation "*i*"		l_{1k}	Length of bottom sleeve for "s_{2i}"
l_{2i}	Distance between bumper and toric stopper in situation "i"		l_{1L}	Length of bottom sleeve for "s_{2M}"
l_{2M}	Maximal value of l_{2i}		l_{1b}	Length of bottom sleeve for "s_{3j}"
p_{2i}	Pressure for position "*i*"		l_{1B}	Length of bottom sleeve for "s_{3M}"
$\alpha_{p2(i)}$	Pressure coefficient in zone 2, position "*i*"		β_{k2i}	Unitary stiffness coefficient in the interval ($i \div i$+1)
$\alpha_{p3(j)}$	Pressure coefficient in zone 3, position "*j*"		$\beta_{k3\,j}$	Unitary stiffness coefficient in the interval ($j \div j$+1)

2. EVOLUTION OF THE SLEEVE ACTUATOR AIR CHAMBER VOLUME WITH THE STROKE

When the actuator is in maximal extension, position represented in Fig. 1a, gas volume has maximal value respectively V_{TM} :

$$V_{TM} = V_{1m} + V_{2M} + V_{3M} + V_S, \tag{1}$$

$$V_{1m} = \frac{\pi}{4}\left[\left(d_S^2 - d_D^2\right)l_{1m} + (d_D^2 - d_{iS}^2)h_{S1}\right] - V_{Ts} - V_{R1}, \tag{2}$$

$$V_{TS} = \frac{\pi}{4}\left[\left(d_{eS}^2 - d_D^2\right)h_{S2} + \left(d_D^2 - d_{iS}^2\right)h_{S1}\right], \tag{3}$$

$$V_{R1} = \frac{\pi}{4}d_R^2 h_{S1}, \tag{4}$$

$$V_{2M} = \frac{\pi}{4}\left(d_S^2 - d_R^2\right)l_{2M}, \tag{5}$$

$$V_{3M} = \frac{\pi}{4}\left(d_S^2 - d_R^2\right)l_{3M} - V_{BM} - V_V, \tag{6}$$

$$V_B = V_{BM} = V_{Bm} = \frac{\pi}{4}\left(d_B^2 - d_R^2\right)\cdot l_{3m}, \tag{7}$$

$$V_V \cong \frac{\pi}{4}d_V^2 \cdot l_V. \tag{8}$$

All the equations the lengths, heights, volumes are signification according Table 1 and Fig. 1.

When actuator compresses with stroke s_{2i} length of zone 2 decreases to l_{2i} and according this the gas volume in zone 1 vary with V_{1k} and volumes in zone 2 are:

$$V_{T2i} = (V_{1m} + V_{1k}) + V_{2i} + V_{3M} + V_S, \tag{9}$$

$$V_{1k} = \frac{\pi}{4}\left(d_S^2 - d_D^2\right)l_{1k} = \frac{\pi}{8}\left(d_S^2 - d_D^2\right)s_{2i}, \tag{10}$$

$$l_{1k} = s_{2i}/2, \tag{11}$$

$$V_{2i} = \frac{\pi}{4}\left(d_S^2 - d_R^2\right) l_{2i}\,. \tag{12}$$

When starts the compression bumper deformation, situation presented in Fig. 1b, the actuator gas volume in zone 2 is zero, and gas volume in zone 3 is maximal V_{3M}, but when the compression continues, the bumper deforms with s_{3j} the gas volume in zone $3\,V_{3j}$ decreases and volume in zone 1 increases with V_{1b}, the total gas volume being V_{T3j}:

$$V_{T3j} = (V_{1m} + V_{1L} + V_{1b}) + V_{3j} + V_S\,, \tag{13}$$

$$V_{1L} = \frac{\pi}{4}\left(d_S^2 - d_D^2\right) l_{1L} = \frac{\pi}{8}\left(d_S^2 - d_D^2\right) l_{2M}\,, \tag{14}$$

$$l_{1L} = l_{2M}\,/\,2\,, \tag{15}$$

$$V_{1b} = \frac{\pi}{4}\left(d_S^2 - d_D^2\right) l_{1b} = \frac{\pi}{8}\left(d_S^2 - d_D^2\right) s_{3j}\,, \tag{16}$$

$$l_{1b} = s_{3j}\,/\,2\,, \tag{17}$$

$$V_{3j} = \frac{\pi}{4}\left(d_S^2 - d_R^2\right)\left(l_{3M} - s_{3j}\right) - V_{Bm}\,. \tag{18}$$

At the full compression bumper deformation presented in Fig.1c the gas volume in zone 3 noted V_{3m} is minimal, the gas volume in zone 1, noted V_{1M}, is maximal and the actuator total gas volume noted V_{T3M} is:

$$V_{T3M} = (V_{1m} + V_{1L} + V_{1B}) + V_{3m} + V_S\,, \tag{19}$$

$$V_{1B} = \frac{\pi}{4}\left(d_S^2 - d_D^2\right) l_{1B} = \frac{\pi}{8}\left(d_S^2 - d_D^2\right)(l_{3M} - l_{3m})\,, \tag{20}$$

$$l_{1B} = (l_{3M} - l_{3m})\,/\,2\,. \tag{21}$$

3. THE PRESSURE EVOLUTION WITH THE STROKE

Considering an isotherm process and p_0 the gas pressure when the actuator is in maximal extension, result:

$$p_0 V_{TM} = p_{2i} V_{T2i} = p_{3j} V_{T3j} = p_{3M} V_{T3m} = p_M V_{Tm}\,. \tag{22}$$

From equation (22) result for working zone 2:

$$p_{2i} = p_0 \frac{V_{TM}}{V_{T2i}} = p_0 \cdot \alpha_{p2i}\ , \tag{23}$$

$$\alpha_{p2i} = \frac{V_{TM}}{V_{T2i}} = \frac{V_{1m} + V_{2M} + V_{3M} + V_S}{(V_{1m} + V_{1k}) + V_{2i} + V_{3M} + V_S}\,. \tag{24}$$

For position $(i+1)$ the pressure has expression below:

$$p_{2(i+1)} = p_0 \frac{V_{TM}}{V_{T2(i+1)}} = p_0 \alpha_{p2(i+1)}\,, \tag{25}$$

$$\alpha_{p2(i+1)} = \frac{V_{TM}}{V_{T2(i+1)}} = \frac{V_{1m} + V_{2M} + V_{3M} + V_S}{(V_{1m} + V_{1(k+1)}) + V_{2(i+1)} + V_{3M} + V_S}\,. \tag{26}$$

From equation (22) result for working zone 3:

$$p_{3j} = p_0 \frac{V_{TM}}{V_{T3j}} = p_0 \alpha_{p3(j)}\,, \tag{27}$$

$$\alpha_{p3(j)} = \frac{V_{TM}}{V_{T3j}} = \frac{V_{1m} + V_{2M} + V_{3M} + V_S}{(V_{1m} + V_{1L} + V_{1b}) + V_{3j} + V_S}\,, \tag{28}$$

$$p_{3(j+1)} = p_0 \frac{V_{TM}}{V_{T3(j+1)}} = p_0 \alpha_{p3(j+1)}\,, \tag{29}$$

$$\alpha_{p3(j+1)} = \frac{V_{TM}}{V_{T3(j+1)}} = p_0 \frac{V_{1m} + V_{2M} + V_{3M} + V_S}{(V_{1m} + V_{1L} + V_{1(b+1)}) + V_{3(j+1)} + V_S}\,. \tag{30}$$

4. THE STIFFNESS EVOLUTION WITH THE STROKE

Stiffness in zone 2, in the interval $2i \div 2(i+1)$ noted $k_{2[i\div(i+1)]}$ is:

$$k_{2[i\div(i+1)]} = \left|\frac{\Delta F_{2[i\div(i+1)]}}{\Delta s_{2[i\div(i+1)]}}\right| = p_0 A_C \left|\frac{\alpha_{p2(i+1)} - \alpha_{p2(i)}}{l_{2(i+1)} - l_{2i}}\right| = p_0 A_C \beta_{k2i}\,, \tag{31}$$

$$\Delta F_{2\left[i\div(i+1)\right]} = A_C\left(p_{2(i+1)} - p_{2i}\right) = p_0 A_C\left(\alpha_{p2(i+1)} - \alpha_{p2i}\right), \tag{32}$$

$$A_C = \frac{\pi}{4}\left(d_S^2 - d_R^2\right), \tag{33}$$

$$\Delta s_{2\left[i\div(i+1)\right]} = l_{2(i+1)} - l_{2i}, \tag{34}$$

$$\beta_{k2i} = \left|\frac{\alpha_{p2(i+1)} - \alpha_{p2(i)}}{l_{2(i+1)} - l_{2i}}\right|, \tag{35}$$

$\Delta F_{2\left[i\div(i+1)\right]}$ – variation of pneumatic force in interval $\left[i\div(i+1)\right]$ of zone 2,

$\Delta s_{2\left[i\div(i+1)\right]}$ – displacement in zone 2 in the interval $\left[i\div(i+1)\right]$.

Stiffness in zone 3, in the interval $\left[j\div(j+1)\right]$, noted $k_{3\left[j\div(j+1)\right]}$ is:

$$k_{3\left[j\div(j+1)\right]} = \left|\frac{\Delta F_{3\left[j\div(j+1)\right]}}{\Delta s_{3\left[j\div(j+1)\right]}}\right| = p_0 A_C \left|\frac{\alpha_{p3(j+1)} - \alpha_{p3(j)}}{l_{3(j+1)} - l_{3i}}\right| = p_0 A_C \beta_{k3j}, \tag{36}$$

$$\Delta F_{3\left[j\div(j+1)\right]} = A_C\left(p_{3(j+1)} - p_{3j}\right) = p_0 A_C\left(\alpha_{p3(j+1)} - \alpha_{p3j}\right), \tag{37}$$

$$\Delta s_{3\left[j\div(j+1)\right]} = l_{3(j+1)} - l_{3j}, \tag{38}$$

$$\beta_{k3j} = \left|\frac{\alpha_{p3(j+1)} - \alpha_{p3(j)}}{l_{3(j+1)} - l_{3i}}\right|, \tag{39}$$

$\Delta F_{3\left[j\div(j+1)\right]}$ – is variation of pneumatic force in interval $\left[j\div(j+1)\right]$ of zone 3,

$\Delta s_{3\left[j\div(j+1)\right]}$ – is displacement in zone 3 for the interval $\left[j\div(j+1)\right]$.

Papers [6–11] show other analyses for sleeve actuators and papers [12, 13] present a new model of pneumatic actuator realised with metallic cylinder.

5. NUMERICAL APPLICATION

We analyze a sleeve actuator model for rear suspension of Dacia Logan MCV car, the specific values being presented in Table 2. This analyse is realised

for the actuator closed, not connected to other devices as gas tanks, accumulators etc. this situation the V_S volume of the supplementary equipments being zero.

$$V_S = 0\,. \tag{40}$$

Table 2

The specific values for rear sleeve actuator for Dacia Logan MCV

Symbol	Value $\times 10^{-2}$	Unit		Symbol	Value $\times 10^{-2}$	Unit
d_S	7	m		l_{1m}	10	m
d_D	4	m		l_{1M}	18.85	m
d_R	1.1	m		l_{2m}	0	m
d_B	4.3	m		l_{2M}	13.7	m
d_{iS}	1.3	m		l_{3m}	4	m
d_{eS}	4.5	m		l_{3M}	8	m
d_V	1.65	m		h_{S1}	0.6	m
l_V	0.9	m		h_{S2}	2	m

According the expressions (23) and (24):

$$p_{2i} = p_0 \alpha_{p2i} = p_0 \frac{1012.37 \cdot 10^{-6}}{498.15 \cdot 10^{-6} + 12.96 \cdot 10^{-4} s_{2i} + 37.53 \cdot 10^{-4} l_{2i}}\,, \tag{41}$$

$$\alpha_{p2i} = \frac{V_{TM}}{V_{T2i}} = \frac{1012.37 \cdot 10^{-6}}{498.15 \cdot 10^{-6} + 12.96 \cdot 10^{-4} s_{2i} + 37.53 \cdot 10^{-4} l_{2i}}\,. \tag{42}$$

According the expressions (27) and (28):

$$p_{3j} = p_0 \alpha_{p3j} = p_0 \frac{1012.37 \cdot 10^{-6}}{679.5 \cdot 10^{-6} - 24.57 \cdot 10^{-4} s_{3j}}\,, \tag{43}$$

$$\alpha_{p3j} = \frac{V_{TM}}{V_{T3j}} = \frac{1012.37 \cdot 10^{-6}}{679.5 \cdot 10^{-6} - 24.57 \cdot 10^{-4} s_{3j}}\,. \tag{44}$$

For the values specified in Table 2, the actuator pressure and stiffness evolution with stoke is according Table 3 and Fig. 2.

In Table 3 the values for pressures and rigidities in ending zone 2, respectively in the position 2_4 are equals with values from starting zone 3, respectively position 3_0.

Table 3

Evolution of the actuator gas pressure and stiffness with stroke

Zone	Actuator Stroke [m]	Position $2i\,;3j$	$s_{2i}\,;s_{3j}$ [m]	$l_{2i}\,;l_{3j}$ [m]	Pressures $p=\alpha_p\cdot p_0$ [Pa]	Stiffness $k=\gamma_S\cdot p_0$ $\gamma_S\,[\mathrm{m}]$
2	0	2_0	0	0.137	$1.00\cdot p_0$	$0.80\times10^{-2}\cdot p_0$ *
	0.040	2_1	0.040	0.970	$1.11\cdot p_0$	$1.00\times10^{-2}\cdot p_0$
	0.080	2_2	0.080	0.570	$1.24\cdot p_0$	$1.25\mathrm{x}\times10^{-2}\cdot p_0$
	0.120	2_3	0.120	0.170	$1.41\cdot p_0$	$1.59\times10^{-2}\cdot p_0$
	0.137	2_4	0.137	0	$1.50\cdot p_0$	$1.93\times10^{-2}\cdot p_0$
3	0.137	3_0	0	0.08	$1.50\cdot p_0$	$1.93\times10^{-2}\cdot p_0$ **
	0.177	3_1	0.040	0.04	$1.74\cdot p_0$	$2.29\times10^{-2}\cdot p_0$

* value was calculated by extrapolation; ** value taken from position "2_4"

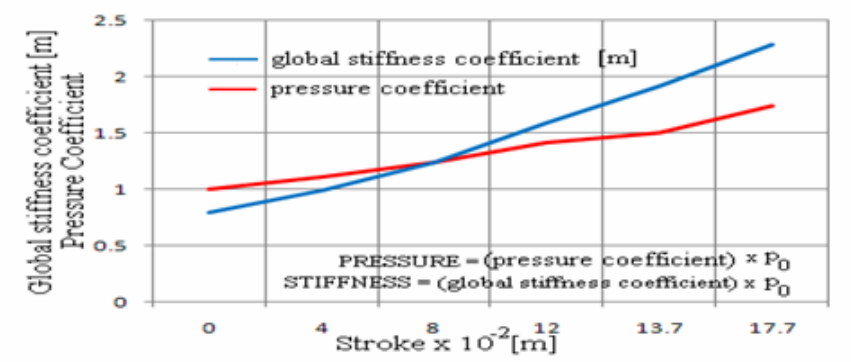

Fig. 2 – Evolution of the actuator gas pressure and stiffness with stroke.

The coefficients α_p and γ_S are signification according Table 4.

Table 4

The pressure coefficient α_p and the global stiffness coefficients γ_S

α_p	pressure coefficient	$\alpha_p=\begin{cases}\alpha_{p2i}\,\text{for}:\, l_{2i}\in(0\div13.7)10^{-2}\,m\\ \alpha_{p3j}\,\text{for}:\, l_{3j}\in(13.7\div17.7)10^{-2}\,m\end{cases}$
γ_S	global stiffness coefficient	$\gamma_S=A_C\beta_k=\begin{cases}A_C\beta_{k2I}\ \text{for}:\, l_{2i}\in(0\div13.7)10^{-2}\,m\\ A_C\beta_{k3J}\ \text{for}:\, l_{3j}\in(13.7\div17.7)10^{-2}\,m\end{cases}$

6. CONCLUSIONS

The paper gives calculus relations for pressure and stiffness evolution with stroke at the sleeve actuator, function of the constructive parameters, necessary in suspension modelling and performances evaluation by simulation. By the pressure control can increase the clearance on bad roads increasing the passing capacity and can decrease it on highway for stability and aerodynamics improving permitting the cruise speed increasing and by the stiffness control can improve the comfort.

Acknowledgements. I acknowledge the support of the Romanian Academy to this paper.

Received on November 26, 2021

REFERENCES

1. ACCUAIR Comp., *Air Suspensions*, https://accuair.com/collections/air-struts
2. CONTITECH Comp., *Sleeve Air Springs*, https://www.continental-industry.com/getmedia/5eda31b0-0264-4e6b-bba2- d7dbaa086758/AS1105-En-Sleeve-Air-Springs.pdf.
3. BILSTEIN, *Air Springs*, https://www.bilstein.com/us/en/airspring/.
4. AIR LIFT Comp., *Bellows vs. sleeves*, https://www.airliftcompany.com/workshop/bellows-vs-sleeve-air-bags/.
5. AMAZON Comp., *Air lift 58130 tapered sleeve air bag*, https://www.amazon.com/LIFT-58130-Tapered-Sleeve-Air/dp/B0021R3DKO.
6. KARIMI ESKANDARY, P., KHAJEPOUR, A., WONG, A., ANSARI, M., *Analysis and optimization of air suspension system with independent height and stiffness tuning,* International Journal of Automotive Technology, **17**, 5, pp. 807−816, 2016, DOI 10.1007/s12239−016−0079−9, pISSN 1229−9138/ eISSN 1976−3832.
7. AHMAD PUAT, A., Z., F., B., *Study of automotive air suspension*, A report submitted in partial fulfillment of the requirements for a degree of bachelor of engineering (Mechanical-Automotive), Honours, 2014.
8. MOHAMMED, M., ALKTRANEE, M., *Parametric analysis of vehicle suspension based on air spring and MR damper with semi-active control*, Journal of Physics: Conference Series 1773, 012022, doi:10.1088/1742-6596/1773/1/012022, 2021.
9. Ho, C., M., TRầN, T., D., NGUYEN, C., H., AHN, K., K., *Adaptive neural command filtered control for pneumatic active suspension with prescribed performance and input saturation*, 2021, doi: 10.1109/ACCESS.2021.3071322.
10. AHMED, M., FATH EL BAB, M., R., El-HUSSIENY, H., Ali, A., *Neuro-fuzzy volume control for quarter car air spring suspension system*, DOI 10.1109/ACCESS.2021.3081872, IEEE Access, 2021.
11. CAO, K., LI, Z., GU, Y., CHEN, L., *The control design of transverse interconnected electronic control air suspension based on seeker optimization algorithm*, Proceedings of the Institution of Mechanical Engineers, Part D: Journal of Automobile Engineering, https://doi.org/ 101177/0954407020984667.
12. NICULESCU, A., I., *"¼ car model for suspension trim corrector performances evaluation"*, Applied Mechanics and Materials, **823**, pp. 205–210, 2016, https://doi.org/10.4028/www.scientific.net/ AMM.823.205 .
13. NICULESCU, A.,I., *On the utilization versions, of the new suspension with trim corrector and their performances*, Acta Electrotehnica, **59**, *1-2*, Special Issue 2344-5637.